RSC Advances

PAPER

View Article Online
View Journal | View Issue

Cite this: *RSC Adv.*, 2015, **5**, 103218

Surfactant-free synthesis of sub-100 nm poly(styrene-*co*-divinylbenzene) nanoparticles by one-step ultrasonic assisted emulsification/polymerization†

Manolis D. Tzirakis,[a] Roman Zambail,[a] Yong Zen Tan,[ab] Jia Wei Chew,[bc] Christian Adlhart[a] and Andrei Honciuc*[a]

Received 11th November 2015
Accepted 23rd November 2015

DOI: 10.1039/c5ra23840d

www.rsc.org/advances

The synthesis of sub-100 nm polymeric nanoparticles in a surfactant-free form is currently very challenging due to the oil nanoemulsion instability in polar solvents and in the absence of stabilizers. Here we report for the first time the surfactant-free synthesis method of poly(styrene-*co*-divinylbenzene) nanoparticles in an aqueous environment using ultrasonic radiation. This method involves emulsification of the monomers mixture in water, followed by free-radical polymerization under pulsed or continuous acoustic fields. The local energy produced in water by cavitation effects was sufficient to: (1) generate and stabilize the monomer nanoemulsion due to mechanical forces, and (2) drive the radical polymerization due to the heat generated. The average size of the final polymer nanoparticles obtained depended: (i) inversely on the monomer/water interfacial energy, emulsification power, and (ii) directly on temperature, amount of initiator and monomer solubility. The polymer nanoparticle size distribution and shape was considerably improved upon the addition of a co-polymerizable surfactant.

1. Introduction

Regardless of composition, nanoparticles (NPs) are acknowledged as key-enablers in the future development of technologies for drug delivery and encapsulation of actives,[1] surface functionalization,[2] fluorescence labeling,[3] smart materials,[4] cosmetics,[5] electronics,[6] and many other applications.[7,8]

Various methods for the synthesis of well-defined polymeric nanoparticles (PNPs) have been reported.[9] The most successful and commonly used method for the preparation of sub-100 nm PNPs is the emulsion polymerization.[10] A major drawback of this method is the need for large amount of surfactants, which are not only costly and environmentally unfriendly chemical agents, but could also be detrimental to the surface properties of the NPs, in the sense that the surfactant-to-nanoparticle ratio cannot be controlled and can change unpredictably due to desorption of the surfactants upon further handling, *e.g.* dilution, or change in ionic strength, *etc.* In most cases, surfactants are difficult to completely remove from the PNPs by standard methods, such as time-consuming serum replacement methods (*i.e.* centrifugation, dialysis, or electrodialysis).[11–16] Surfactant-free NPs could find use in a variety of fundamental studies, for example, toxicological evaluation of NPs for medical applications; such tests could be invalidated by the presence of surfactants that carry their own toxicological fingerprint.[11,17,18] The absence of surfactants is also important for applications heavily relying on consistent, reproducible surface properties of NPs. Furthermore, surfactant-free NPs are important for interfacial activity studies, such as generation of Pickering emulsions and surface functionalization *via* the Langmuir–Blodgett methods.

In this work we report for the first time the ultrasonic assisted synthesis of surfactant-free poly(styrene-*co*-divinylbenzene) NPs with average sizes below 100 nm in an aqueous environment. While the micron-sized surfactant-free NPs, *i.e.* poly(styrene-*co*-divinylbenzene), can be prepared by precipitation polymerization,[19–23] this is not applicable for preparing sub-100 nm PNPs. Small NPs, *i.e.* in the sub-100 nm range, exhibit increased surface-to-volume ratio which endows them with increased capacity to absorb molecules on their surface, and hence increased potential for several applications such as, for example, drug delivery, water treatment, and catalysis. The use of ultrasonic radiation is not new, especially in emulsification, emulsion polymerization[24] and synthesis of inorganic particles,[25–29] but it has not been applied to simultaneously

[a]*Institute of Chemistry and Biological Chemistry, Zurich University of Applied Sciences, Einsiedlerstrasse 31, 8820 Waedenswil, Switzerland. E-mail: andrei.honciuc@zhaw.ch; Tel: +41 589345283*

[b]*School of Chemical and Biomedical Engineering, Nanyang Technological University, Singapore 637459, Singapore*

[c]*Singapore Membrane Technology Center, Nanyang Environment and Water Research Institute, Nanyang Technological University, Singapore 637141, Singapore*

† Electronic supplementary information (ESI) available. See DOI: 10.1039/c5ra23840d

emulsify, initiate and drive a radical polymerization reaction to generate surfactant-free PNPs. Ultrasonic irradiation allows for the preparation of stable emulsions without the need for surfactants, simply by the use of mechanical forces generated from acoustic cavitation at the liquid/liquid phase boundaries.[30–35] Acoustic (ultrasonic) emulsification is regarded as a powerful method for the rapid production of environmentally benign emulsions,[35–38] which upon further treatment under polymerization conditions can afford surfactant-free PNPs.[37,39–41] Atobe and co-workers have recently demonstrated the utility of this approach in the synthesis of size-controlled polymethylmethacrylate (PMMA) NPs *via* a two-step process, involving first a sequential acoustic emulsification of methylmethacrylate (MMA) in water using different ultrasonic devices of different frequencies, followed by non-acoustic polymerization of the monomer droplets in the obtained solution.[37,38,41]

Here we exploit the potential of the acoustic emulsification technique in the preparation of surfactant-free PNPs, particularly poly(styrene-*co*-divinylbenzene) [P(St/DVB)] NPs. Towards this goal, we developed a new, one-step acoustic emulsification/polymerization method, and we systematically investigated the effect of different parameters, such as (i) the total concentration of the monomer/crosslinker and their relative ratio, (ii) the nature and the amount of the initiator, (iii) the reaction temperature and time, and (iv) the addition of stabilizer at different concentrations, on the size and size distribution of the PNPs.

2. Experimental section

2.1. Materials and methods

All reagents and solvents were purchased from commercial suppliers and used as received unless otherwise noted. Styrene (St; Reagent Plus, 99%), divinylbenzene (DVB; technical grade, 80%), poly(vinyl alcohol) (PVA; 13 000–23 000 g mol^{-1}, 87–89% hydrolyzed), poly(ethylene glycol) (PEG400; average $M_n = 400$), and ammonium persulfate (APS; ACS reagent ≥98.0%) were supplied by Sigma-Aldrich. 2-Sulfoethyl methacrylate (2-SEM; >90%) was purchased from Polysciences, Inc. 2,2′-Azobis(2-methylpropionitrile) was purchased from Aldrich and recrystallized from methanol and dried before use. Monomers (St and DVB) were filtered through a basic alumina column to remove the inhibitor before use. Purified St and DVB were stored in a freezer prior to use. All solvents were of HPLC grade. Ultrapure water (UPW; resistivity, ρ, at 298 K: 0.055 μS cm^{-1}, or 18.2 MΩ cm) was obtained from an Arium 611 VF water purification system (Startorius stedim biotech, Aubagne, France), and it was used as the aqueous medium in all experiments.

2.2. Acoustic emulsification/polymerization

2.2.1. Experimental procedure. Unless otherwise stated, all experiments in the present study were carried out according to the experimental protocol described as follows. St/DVB (1 : 1, v/v; 200 μL) and APS (50 mg; 0.22 mmol, 6.2 mM) were added to ultrapure water (UPW; 18 MΩ cm) (35 mL) in a Falcon® polypropylene (PP) conical tube (50 mL) to give a mixture of low monomer content (~0.6 wt%). This oil-in-water mixture was then subjected to ultrasonication under argon atmosphere by using a Branson Sonifier W-450 Digital (20 kHz, 400 watt) equipped with a 3/4″ (19 mm) titanium horn, with amplitude of 70% for 60 min (Fig. S1†). The horn was positioned 4 cm below the surface of the reaction mixture. During ultrasonication the vial was immersed in an ice/water bath to counteract the considerable heating resulting from ultrasonication and maintain the temperature of the reaction mixture at 80 °C. After the reaction was over, the crude samples were centrifuged for 20 min at 3000 rpm for removal of coagula. The supernatant was further purified by three centrifugation steps to ensure complete removal of monomers, initiator, and other trace impurities. In the first centrifugation step the supernatant was centrifuged at 13 000 rpm for 60 min. In the second step, the generated white sediment was re-dispersed in UPW and was further centrifuged at 13 000 rpm for 60 min. Finally, in the last step the sediment was washed with acetonitrile (13 000 rpm, 60 min). The isolated yields of pure P(St/DVB) NPs were in the range 6–9%.

2.2.2. Acoustic power and heat dissipation. The calorimetric method is the standard way of evaluating the ultrasonic power input to the solution, and it assumes that all the energy delivered to the system is eventually thermalized and dissipated as heat.[42] For this purpose a thermocouple was inserted through a custom-made side arm of a Falcon® polypropylene conical tube (50 mL) such that its tip was positioned at *ca.* 2 cm below the 3/4″ acoustic horn. 38.35 g of UPW were weighed on an analytical scale and added into the above tube. After ample equilibration, the temperature was 23.1 °C. The ultrasonication power amplitude was set at 70% and started for a fixed duration of 30 s. The actual temperature in the reaction tube and the power output, *i.e.* power applied to the horn (read from the display), were noted every second. The temperature at the end of ultrasonication was 37.6 °C. The total heat transfer was calculated with the equation: $Q = c \times m \times \Delta T$, where c is the specific heat capacity of water (4.1804 kJ K^{-1} kg^{-1}), m is the mass of the UPW used, and ΔT is the temperature change. The temperature change of the polypropylene Falcon® tube was negligible after 30 s of ultrasonication and therefore was neglected from our calculations. The total heat generated as determined by the calorimetric method was 2325 J (77.5 W) while the power output to the horn as read from the display was 4440 J (148 W), which hence yields a 52% electric-to-acoustic conversion efficiency. Because the calorimetric experiments were carried in non-adiabatic conditions, *i.e.* the horn, and thermocouples acting as heat-sinks, the experiment was repeated for shorter times, *i.e.*, 15 s, to approach the adiabatic limit. The results obtained at shorter times were comparable, but with a slightly lower electric-to-acoustic conversion efficiency of 44%, which suggests that the horn immersed in the solution acted as a heat source rather than a heat-sink. At this point, it should be noted that heating comes mostly from sonication, and not from enthalpy of polymerization, since the low monomer content of the present system (~0.6 wt%) cannot generate appreciable heat.

2.3. Nanoparticle characterization

For SEM measurements, the centrifuged samples were diluted in ultrapure water, mounted on aluminum stubs, dried at 80 °C for 4 hours, and sputter-coated with a thin layer of gold (approx. 4 nm) to increase their conductivity and prevent charging. The sputter-coater (Q15OR-S Sputter Coater, Quorum) was operated at 20 mA for 30 s, under Ar atmosphere (sputter vacuum: 5×10^{-2} mbar). The gold films deposited on our samples caused an increased roughness on the particles' surface with typical characteristic structures composed of small rounded grains and also small and densely packed isolated islands or clusters up to $d \approx 4$ nm. Non-sputtered samples were also imaged for comparison (for example see Fig. S5 in ESI†). All SEM images were acquired on a FEI Quanta FEG 250 scanning electron microscope, operating at 5–30 kV accelerating voltage in the secondary electron (SE) mode, at high vacuum (3×10^{-6} to 1.8×10^{-5} mbar). All image analyses were conducted using open source software ImageJ (NIH, US). Dynamic Light Scattering (DLS) measurements were performed on a Malvern Zetasizer Nano-ZS instrument (Malvern Instruments, Worcestershire, UK) equipped with a 4 mW He–Ne laser at a wavelength of 633 nm at a scattering angle of 173° and at 25 °C, using standard polystyrene disposable cuvettes. All samples were thermally equilibrated to 25 °C for 3 min prior to acquiring 3 sets of DLS measurements. The number-average particle diameter ($\bar{d}_N$) and particle-diameter dispersity ($Đ_d$)[43] were calculated from SEM pictures of the samples by measuring the diameters of approximately 200 particles (randomly chosen from high-quality SEM images). The zeta potential of surfactant-free P(St/DVB) NPs could not be determined due to fast sedimentation of these particles upon purification and redispersion in UPW.

2.4. Interfacial tension measurements

The interfacial tension (IFT) measurements were carried out through the evaluation of the equilibrium drop shape using a DataPhysics OCA 15Pro contact angle goniometer equipped with an automatic dosing system. The IFT was measured by analyzing the contour of a pendant drop. The images of the drop shape were captured in real time and then digitally analyzed using edge-detecting DataPhysics SCA 22 software module by fitting the contour of the droplet to the Young–Laplace equation. For all interfacial measurements 20–25 μL St/DVB droplets were generated at the apex of an upward-bended dosing needle within an aqueous phase contained in a 20 cm cubic quartz cuvette. The IFT of a St/DVB droplet (of varying monomer ratios 5 : 95 → 95 : 5) was measured in the following ambient phases: UPW, 1 wt% of 2-SEM, PEG, PVA and finally CTAB in UPW. Due to the high sensitivity of the measuring method, a strict experimental procedure was followed. All mixtures were prepared and used within 10 h of preparation to avoid contamination. The quartz cuvette used to contain the ambient phase was rinsed with ethanol and acetone then allowed to dry, before rinsing once with the appropriate liquid/mixture for the next set of experiment. The Hamilton syringe and dosing needle used to produce the drop phase in the ambient phase were rinsed with ethanol and acetone then allowed to dry, before rinsing once with the appropriate St/DVB mixture for the next set of experiment.

3. Results and discussion

3.1. Acoustic emulsification and preparation of monomer nanodroplets

The acoustic emulsification of the mixture of water-insoluble monomers, namely, St and DVB, in an aqueous medium was first studied. In these experiments, St/DVB (1 : 1, v/v; 200 or 300 μL) was added to UPW (35 mL) in a Falcon® polypropylene (PP) conical tube (50 mL). The 20 kHz ultrasonication of the oil-in-water mixture was conducted with an ultrasonic disruptor horn (tip diameter: 3/4″) connected with a 20 kHz oscillator for 5, 10, 15, 20, 30, 40, 60 and 80 min. To quantitatively evaluate the size of oil droplets and their size distribution, dynamic light scattering (DLS) measurements were performed after each acoustic emulsification treatment. Fig. 1a further shows that longer ultrasonication time results in decreasing mean droplet

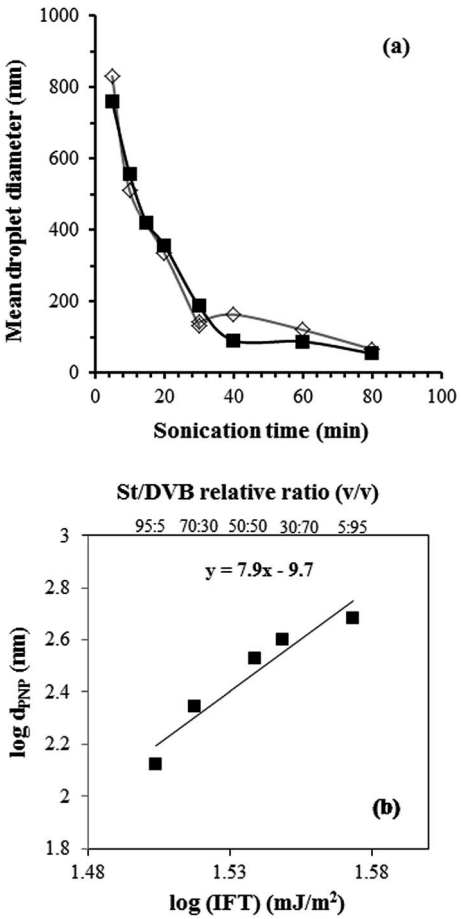

Fig. 1 (a) Mean droplet size of the emulsion produced after acoustic treatment of two different St/DVB (1 : 1, v/v) monomer concentrations (◇) 5.7×10^{-3} L L^{-1} and (■) 8.6×10^{-3} L L^{-1} with acoustic treatment time; (b) mean droplet size with varying the monomer relative ratio St/DVB (95 : 5 → 5 : 95, v/v) and interfacial tension after 20 min ultrasonic irradiation of a 5.7×10^{-3} L L^{-1} monomer solution.

diameter. A milky white solution was observed immediately after beginning the ultrasonic treatment and its appearance gradually changed to a transparent emulsified solution with increasing the sonication time (Fig. S2 in the ESI†). The degree of emulsion transparency can be qualitatively associated with a decrease in oil droplet size. Also, we observed visually that the transparent appearance of the final emulsified solutions was maintained for several weeks, thus confirming the stability of such ultrasonic-derived emulsions over time, even under surfactant-free conditions.[36–38] The observed stability after >20 min of ultrasonification should be ascribed, at least in part, to the very low oil content of the present emulsion system. On the other hand, the translucent or white milky emulsions obtained after 5 min of sonication were not stable, due to the presence of larger droplets that are susceptible to fast coalescence and complete phase separation, which occurred within a few hours. Similarly, at sonication times of 10–15 min we observed emulsion breakdown *via* a creaming process over several hours. Fig. 1a shows the change in the ND average size for two different monomer St/DVB (1 : 1, v/v) concentrations, namely 5.7×10^{-3} L L^{-1} and 8.6×10^{-3} L L^{-1}, as a function of acoustic irradiation of up to 80 min. The ND average size decreases steeply between 0–40 min followed by a plateau at longer treatment times, *i.e.* >50 min, after which the size of the oil droplets remain stable at around 100 nm; presumably, further breakdown of NDs into smaller size competes with their fast coalescence or Ostwald ripening. The emulsification by ultrasonic irradiation was repeated for varying ratios of St/DVB (95 : 5 → 5 : 95, v/v) and fully detailed in Fig. S2.†

Interestingly, an increase of the DVB relative ratio in the St/DVB mixture (95 : 5 → 5 : 95, v/v) resulted in increase of the mean droplet diameter (Fig. 1b & S3†), which can be explained by the monotonic increase of the water/ND interfacial energy from *ca.* 32 mN m^{-1} (St/DVB 95 : 5, v/v) to 37.5 mN m^{-1} (St/DVB 5 : 95, v/v), also shown in Table 1. The fact that the maximum ND size increases with increasing IFT up to a critical diameter that is characteristic of the particular system is best described by eqn (1):

$$d_{\max} \approx C \times \varepsilon^{-2/5} \times \gamma^{3/5} \times \rho^{-1/5} \quad (1)$$

where ε – is the total energy dissipated per unit volume, γ – is the interfacial tension, ρ – is the density of a continuous phase and C is a constant typically of the order of unity.[44] Eqn (1) is derived from the Kolmogorov's theory of minimum dissipative structure and it sets an upper limit for the largest oil droplets that can be obtained in an emulsion.

3.2. One-step acoustic emulsification/polymerization under surfactant-free conditions

The ultrasonic emulsification of monomers in the absence of radical initiators is summarized in Fig. 1. Although polymerization may also occur, *via* thermally[45,46] or sonochemically generated[40,47–49] free radicals, the control experiments showed that the polymerization of St and DVB was negligible under the present conditions in the absence of any chemical radical initiators, for emulsification times of up to 60 min.

With the addition of chemical initiators, such as APS, to the emulsified monomer and extending the ultrasonic irradiation duration for another 60 min, PNPs were obtained under surfactant-free conditions. In order to evaluate the performance of this method, a series of experiments were conducted in which the effect of various parameters, namely, the total concentration of the monomer/crosslinker and their relative ratio, the nature and concentration of the initiator, the reaction temperature, the ultrasonication time, and addition of stabilizers, were systematically investigated. It should also be noted that, in the present work, ultrasonic irradiation was applied throughout the polymerization process in order to prevent coagulation/aggregation between NPs in the absence of surfactants while, concurrently, the generated local heat drove the APS-initiated polymerization reaction. Control experiments were also ran under pulsed acoustic field, or under short acoustic treatment (10 min) followed by non-acoustic, thermal polymerization at 80 °C under mechanical stirring.

3.2.1. Effect of the monomer-to-crosslinker relative ratio and their overall concentration. The effect of the relative ratio of monomers, *viz.* monomer (St)-to-crosslinker (DVB) ratio, was studied by conducting a series of polymerization experiments in which the DVB content was gradually increased from 5% to 95% while keeping all the other parameters constant, as described in the Experimental Section (2.2.1). As shown in Fig. 2, the mean size of P(St/DVB) NPs decreases with increasing the DVB content; this effect becomes more pronounced, especially when comparing the two extreme cases where the proportion of St or DVB in the total monomers volume was only 5% (Fig. 2a and e). One might be tempted to hypothesize that this decrease in the particle size should reflect the higher crosslinking degree of P(St/DVB) NPs with increasing DVB content, because it has been previously recognized that a higher crosslinking degree leads to a reduced particle volume or porosity, which is also less prone to solvent intake, *i.e.* swelling.[50] However, this hypothesis would only hold if one makes the assumption that the initiation starts right in the droplet, *i.e. via* a heterogeneous nucleation mechanism, and that the starting ND dimensions for varying monomer ratios are all similar, which is rather not supported by the emulsification data (Fig. S3†). This hints at a possible homogeneous-like nucleation mechanism, which will be further discussed in Section 3.2.5. The presence of some particles with irregular shape, also points to a possible aggregation process during polymerization under surfactant-free conditions. In fact, this observation supports the operation of an aggregation nucleation mechanism further discussed in Section 3.2.5.

The data presented in Fig. S4† shows that the average size P(St/DVB) NPs prepared *via* acoustic emulsification/polymerization at constant monomer-to-crosslinker relative ratio, was independent of monomer concentration within the range from 1.4×10^{-3} to 8.6×10^{-3} L L^{-1}. This is most likely due to the fact that at longer ultrasonication times, exceeding 40 min, the size of the ND produced remained stable at *ca.* 100 nm, regardless of the monomer

concentrations and at a fixed monomer-to-crosslinker composition, as observed in Fig. 1a. On the other hand, improvement of the diameter dispersity $Đ_d$ was observed for the PNPs obtained from the lowest monomer concentration ($Đ_d = 1.07$) as compared to the same PNPs obtained at higher monomer concentrations ($Đ_d = 1.17 - 1.3$). This effect should be ascribed, at least in part, to the lower concentration of polymerization nuclei, which prevents coalescence of the growing oligomers and particles, thus resulting in a decrease of dispersity; further mechanistic details are provided in Section 3.2.5.

For the sake of comparison P(St/DVB) NPs were prepared by following an alternative procedure that avoids continuous sonication of the reaction mixture. In particular, this procedure included the acoustic emulsification for 10 min, followed by radical polymerization at 80 °C for 24 h, with heat provided by a heating plate and under magnetic stirring conditions. The SEM image in Fig. S6† shows that the thermally prepared NPs appear considerably fused, or aggregated, which is in clear contrast to those prepared *via* a continuous acoustic emulsification/polymerization process wherein aggregation is much less pronounced (Fig. 2c). Furthermore, the presence of large aggregates in Fig. S6† is most likely due to increased coalescence of the growing PNPs in the absence of surfactant. The comparison of the data between Fig. 2c and S6,† underlines the advantage of keeping the acoustic pulse throughout the polymerization reaction.

3.2.2. Effect of the nature and the amount of initiator. The impact of the type and concentration of the initiator on polymerization was also investigated. The two initiators tested were ammonium persulfate (APS) and azobisisobutyronitrile (AIBN). The concentrations tested were such that the molar ratios of the initiator to total monomer concentrations were 3%, 7%, 14% and 28% (corresponding to 1.2 mM, 2.9 mM, 6.3 mM, and 12.5 mM, well within the range of literature reported values[51]), and the acoustic emulsification/polymerization was carried out according to the standard experimental procedure, detailed in Section 2.2.1.

APS is a water-soluble radical initiator commonly used in emulsion polymerization. Fig. S7† shows the effect of the various APS concentrations on the size and the diameter dispersity of P(St/DVB) NPs. With increasing APS concentrations in the range investigated, the NP average size increased from 41 to 67 nm. Interestingly this observed trend is opposite from the one reported by Goodwin *et al.* for synthesis of PS lattices in the absence of surfactants, in which case, however, all experiments were conducted under mechanical stirring and at constant ionic strength.[52] In agreement with our results, previous studies have shown that the average particle size increases with increasing initiator concentration in reactions where the ionic strength is not controlled.[53] It should be noted that the herein observed trend cannot be the result of the polymerization being initiated directly inside the existing monomeric NDs, but hints at a coagulative nucleation mechanism further discussed in Section 3.2.5.[54] At this point it is worth noting the dual role of APS, which, in addition to initiating the radical polymerization, also serves as a particle stabilizer due to the charged sulfate groups. This may explain the need for

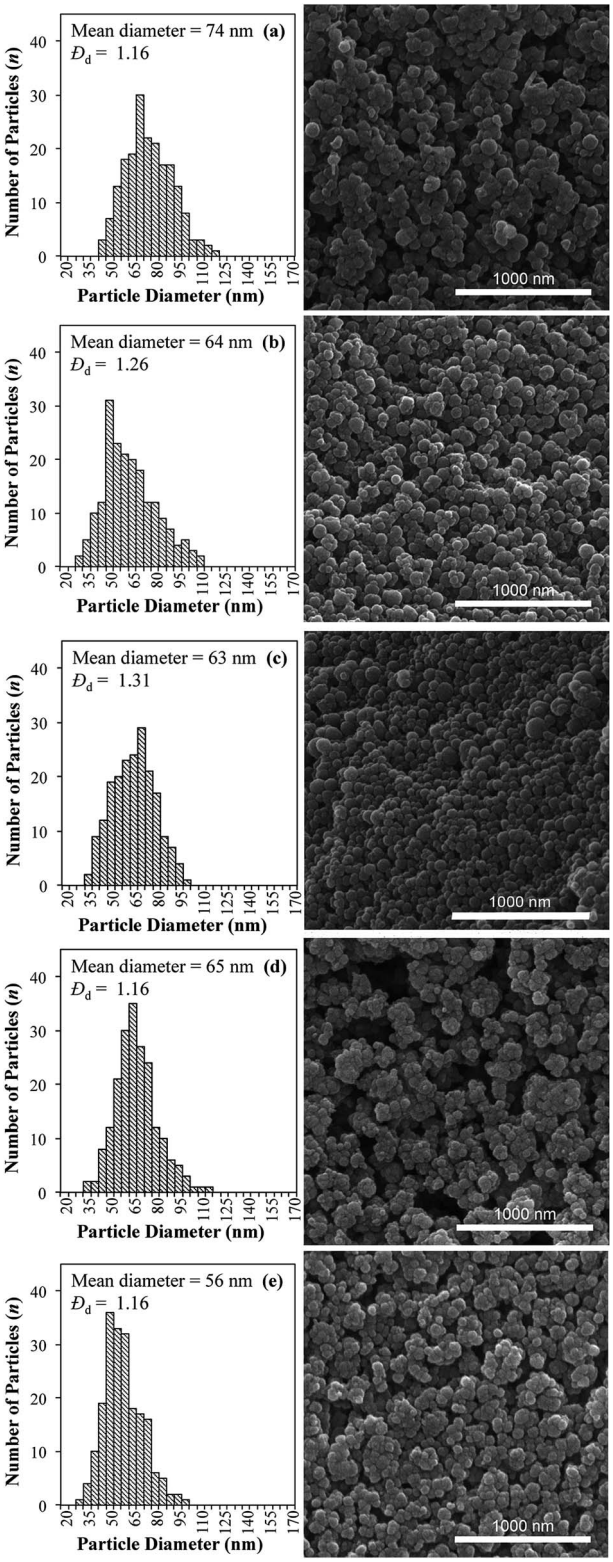

Fig. 2 SEM images and corresponding particle size histograms of P(St/DVB) NPs prepared *via* acoustic emulsification/polymerization of St/DVB monomer, 5.7×10^{-3} L L^{-1} in UPW for 60 min, at different volumetric St : DVB ratios: (a) 95 : 5, (b) 70 : 30, (c) 50 : 50, (d) 30 : 70, and (e) 5 : 95. All samples were sputter-coated with a thin layer of gold (approx. 4 nm; for further details see Section 2.3) prior to SEM imaging.

using a relatively high APS : monomer ratio in the present system, since the surfactant-free emulsion polymerization of very apolar monomers (such as St/DVB) needs an appreciable amount of ionic initiator to stabilize the polymer particles during polymerization. In other words, the greater ionic strength of the aqueous phase, which increases with increasing APS content, is expected to result in an increase of the PNPs' diameter;[53] this was previously explained in terms of a limited coagulation process occurring at the stage involving the nucleation of polymer particles, which will be further discussed in Section 3.2.5.[52,55] In terms of the lowest particle-diameter dispersity, the optimum concentration of APS was 6.3 mM.

Azobisisobutyronitrile (AIBN) was also tested as an alternative, oil-soluble initiator, under the above reaction conditions[39] and at concentrations somewhat larger compared to those reported[56] in literature. The yield of PNPs when using AIBN was very low and very few nanoparticles could be detected by SEM.

3.2.3. Effect of reaction temperature and time. The effect of reaction temperature on the particle size and size distribution of the P(St/DVB) NPs was also probed. It was initially expected that, when the reaction temperature decreases (*i.e.* from 80 to 60 °C), the size of the PNPs increases proportionally.[52] In particular, the particles' size should be directly affected by the concentration of primary free radicals produced by the initiator (APS) at short times, which is a function of the reaction temperature. Assuming a homogeneous nucleation mechanism, the lower the temperature, the lower the number of free radicals produced at short times (as compared to higher temperature), which, in turn, should result in less primary nuclei and hence bigger P(St/DVB) particles. However, as seen in Fig. 3, the mean size of NPs generated at 60 °C is clearly decreased (47 nm) compared to that when the same reaction was performed at 80 °C (63 nm; Fig. 2c). Interestingly also in this case, the observed trend with temperature is opposite from the one reported by Goodwin *et al.* for synthesis of PS lattices in the absence of surface active agents under mechanical stirring.[52] We assume that decrease in temperature mainly results in an increase in oil–water interfacial tension and also in decreased diffusion of apolar monomers, *i.e.* St and DVB, into the aqueous phase. This effect should not only disfavor the rate of a homogeneous nucleation mechanism at the early stage of polymerization, but should also disfavor the following stage of NPs growth *via* aggregation and swelling with monomer (see also the discussion in Section 3.2.5), thus resulting in smaller P(St/DVB) particles. Another possible explanation for the observed trend should be associated with the greater cavitation effect in water, which increases with decreasing temperature within a certain temperature range.[42] Although the cavitation effect is not easily quantifiable, the stronger cavitation at 60 °C *vs.* 80 °C prevents the aggregation of radical oligomers or the coalescence of the growing particles, thus resulting in smaller particles *via* an aggregation nucleation mechanism (see Section 3.2.5).

It should be noted that the emulsification/polymerization temperature was successfully maintained at 60 °C by operating the sonifier in a pulsed mode, wherein ultrasonics are applied at time intervals automatically adjusted by a temperature feedback loop in order to keep the reaction temperature constant at 60 °C. For comparison and consistency with the corresponding experiments performed at 80 °C, the reaction at 60 °C was allowed to run for 150 min of overall reaction time, which is equivalent to 60 min of effective ultrasonication time.

To study the effect of reaction duration on PNP size the emulsification/polymerization reaction was carried under the standard condition (Section 2.2.1) and was stopped at different times between 20–90 min. As an example, Fig. S8† shows a sample of P(St/DVB) NPs obtained at shorter reaction time (20 min). The mean PNP diameter obtained at 20 min is comparable to that obtained after 60 min of reaction, but the heterogeneity of the sample appears to be significant, with many small clustered NPs. Further such controlled experiments confirmed that the optimum reaction time is between 50 and 70 min, above which the yield and diameter dispersity of P(St/DVB) NPs is not further improved.

The impact of ultrasonication amplitude, which determines the strength of cavitation in the sample, was also investigated with all other reactions parameters kept constant. When the ultrasonication amplitude was lowered from 70% to 30%, an increase in the size and diameter dispersity of the P(St/DVB) NPs was observed (Fig. 4). An increase in the NP diameter with the reduction in ultrasonic power was also predicted by eqn (1). In addition, lower ultrasonication amplitude is expected to disfavor the growing of NPs *via* an aggregation nucleation mechanism (Section 3.2.5) thus resulting in smaller NPs. It should also be noted that high ultrasonic intensities can promote some undesired effects, such as NPs degradation. At high ultrasonic intensities (>70%) or extended reaction times (>90 min), we observed the formation of a small amount of a dark material which we were not able to identify or characterize. Control experiments in the absence of St/DVB and/or APS did not show the formation of this material, the origin of which should thus be associated to the P(St/DVB) NPs produced during the present emulsification/polymerization protocol. Another possible explanation for the formation of this small amount of dark material at high ultrasonic intensity is the

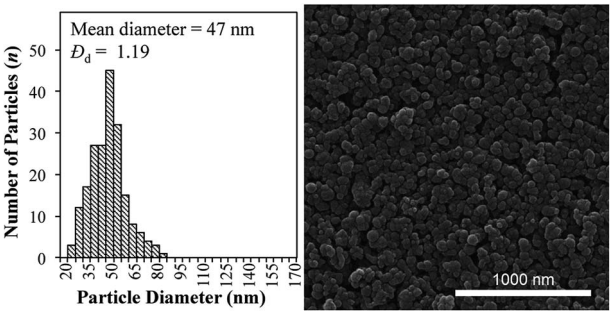

Fig. 3 SEM image and particle size histogram of P(St/DVB) NPs prepared *via* pulsed acoustic emulsification/polymerization of a 1 : 1 mixture of St/DVB (200 μL; 5.7×10^{-3} L L^{-1}) in UPW (35 mL) at 60 °C. The sample was sputter-coated with a thin layer of gold (approx. 4 nm; for further details see Section 2.3) prior to SEM imaging.

abrasion from the sonicator tip, possibly as a result of a redox reaction during the APS-assisted radical polymerization.

3.2.4. Effect of stabilizer concentration. In the absence of stabilizers, the aforementioned P(St/DVB) NPs diffuse randomly in the dispersing liquid phase and the system is susceptible to agglomeration. Indeed, DLS analysis showed that after these surfactant-free NPs are purified and dried to powder form, their complete redispersion in UPW is difficult even upon thermal treatment, vigorous magnetic stirring, and/or tip- or bath-sonication. Also, most of our samples exhibited polydispersed particle sizes and, in some cases, poorly defined morphologies or irregular shape (Fig. 2–4, and S4–S8 in ESI†). With the use of interfacial stabilizers we were able to better control particle growth, enhance colloid stabilization, and prevent agglomeration of the obtained PNPs. In the present study, we tested three categories of stabilizers: (i) water-soluble, steric-based stabilizers with low interfacial activity, namely, polyvinyl alcohol (PVA), and polyethylene glycol (PEG); (ii) a cationic surfactant, namely, cetyltrimethylammonium bromide (CTAB), which has been previously employed as stabilizer in the microemulsion polymerization of styrene,[57,58] and (iii) a water-soluble monomer, namely 2-sulfoethyl methacrylate (2-SEM), in order to introduce polar sites into our P(St/DVB) chains, and also to confer shear stability to our aqueous polymer dispersions. All experiments were carried out under standard conditions described in the experimental procedure (Section 2.2.1), with an extra addition of a 1 wt% stabilizer into the water phase.

Fig. 5 shows the SEM images of the different samples obtained by employing different stabilizers. It should be noted that SEM images were recorded after repeated washings of all samples with water and ethanol or acetonitrile to remove residual stabilizers. The presence of stabilizers in the reaction mixture had a substantial effect on both the size and dispersity of the isolated PNPs, such that their mean diameter was considerably larger than that of the non-stabilized particles (63 nm; see Fig. 2c), with the exception of CTAB (50 nm; see Fig. 5a).

Only in the case of PEG ($Đ_d = 1.09$) and, most importantly, in the case of 2-SEM ($Đ_d = 1.08$) there was a significant improvement of the diameter dispersity of these NPs as compared to their non-stabilized analogues ($Đ_d = 1.31$). In this latter case, preliminary FTIR analysis showed intense ν(S═O), ν(C–O), and ν(C═O) absorptions at *ca.* 1170, 1200, and 1710 cm^{-1}, respectively, confirming the incorporation of 2-SEM units in the bulk and/or the surface of P(St/DVB) NPs (Fig. S9 and S10†).

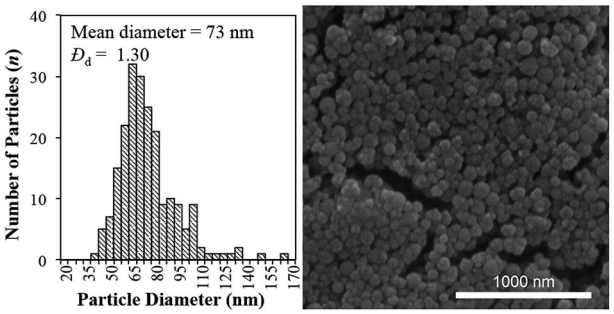

Fig. 4 SEM images and particle size histogram of P(St/DVB) NPs obtained upon standard reaction conditions at lower ultrasonic amplitude (30%). The sample was sputter-coated with a thin layer of gold (approx. 4 nm; for further details see Section 2.3) prior to SEM imaging.

To further probe the potential of ultrasonic irradiation for the preparation of P(St/DVB) NPs in the presence of stabilizers, we repeated the above reaction, in the presence 2-SEM, by following an alternative procedure that avoids continuous sonication throughout polymerization. In this case, ultrasonic irradiation was applied only for 10 min, after which ultrasonication was ceased and the reaction mixture was stirred at 80 °C for 12 h. A SEM image of this sample after purification is presented in Fig. S11.† These particles showed substantial differences in size ($\bar{d}$ = 92 nm) and diameter dispersity ($Đ_d$ = 1.18) as compared to those particles prepared *via* a continuous acoustic emulsification/polymerization process ($\bar{d}$ = 72 nm, $Đ_d = 1.08$; Fig. 5b) which further emphasizes the advantage of maintaining the ultrasonication throughout the polymerization process. The isolated yield of this reaction was 6.3%, which is lower in comparison to the corresponding yield of P(St/DVB) NPs obtained *via* the stabilizer-free method, 8.5%, presumably because the higher solubility of these stabilized PNPs hampers their isolation and purification through repeated centrifugation/re-dispersion cycles.

3.2.5. Mechanistic considerations. The mechanism of surfactant-free emulsion polymerizations has attracted significant scientific interest for over 40 years.[51,54,59–68] A large body of literature studies suggest that the particle nucleation mechanism in surfactant-free emulsion polymerization occurs mainly *via* a coagulative or aggregation nucleation (homogeneous nucleation accompanied with coagulation or limited flocculation) mechanism.[51,54,61–68] The initial stage of polymerization involves the formation of water-insoluble polymer chains which collapse to form precursor particles. These precursor particles are too unstable to remain isolated, since they possess only a small number of charged initiator residuals on their surface to stabilize them. Thus, they coagulate to produce stable particles or they form small aggregates until they achieve enough surface charge to be individually stable. Such aggregates can then swell with monomer and form mature particles.[68] The use of ultrasonication throughout the polymerization process inevitably makes the particle nucleation and growth mechanisms more complicated. However, as will become apparent from the discussion further below, such a coagulative nucleation mechanism is probably operating also in the present system.

The experimental evidence, summarized in Fig. 6a and d, shows that the average diameter of the PNPs generated *via* acoustic emulsification/polymerization depend inversely on the precursor NDs size, which is a strong indication that radical initiation and polymerization did not take place directly in the emulsion monomer droplets. A homogeneous nucleation accompanied with coagulation mechanism,[51,54,61–68] based on the premise that the radical initiator will first react with the St and DVB monomers available in the aqueous phase, may best explain the mechanism of acoustic polymerization in the current work. The homogeneous nucleation hypothesis also finds support in the following experimental observations: (1)

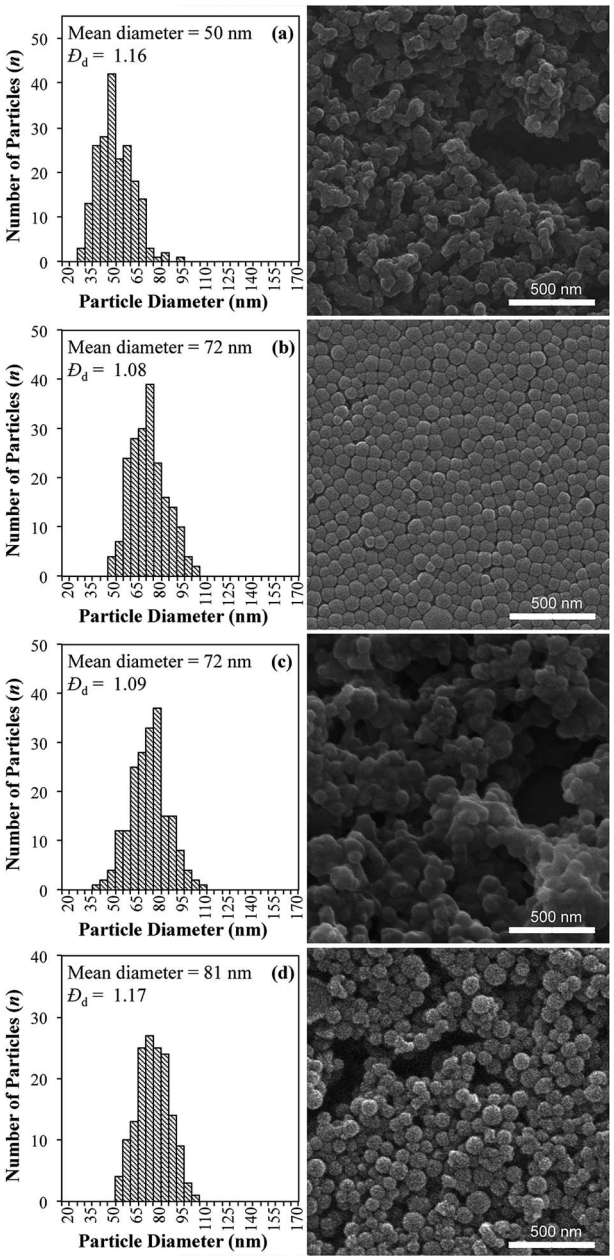

Fig. 5 SEM images and particle size histograms of P(St/DVB) NPs synthesized in the presence of different stabilizers: (a) cetyltrimethylammonium bromide (CTAB), (b) 2-sulfoethyl methacrylate (2-SEM), (c) poly(ethylene glycol) (PEG400), (d) polyvinyl alcohol (PVA). All samples were sputter-coated with a thin layer of gold (approx. 4 nm; for further details see Section 2.3) prior to SEM imaging.

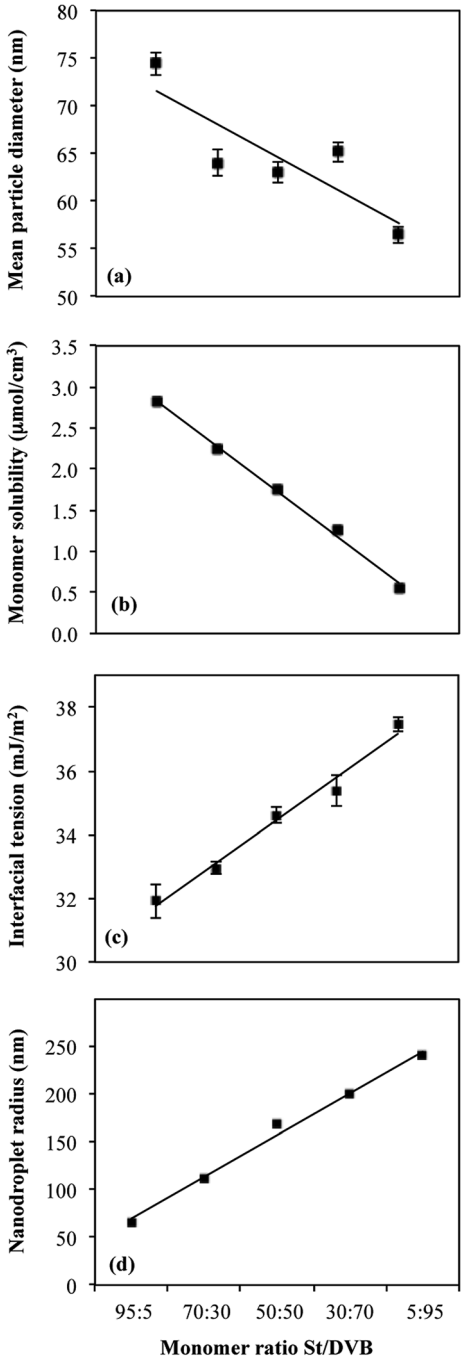

Fig. 6 Graphical plot of: (a) mean particle diameter (nm), (b) monomers solubility (μmol cm^{-3}), (c) interfacial tension (mJ m^{-2}) and (d) nanodroplet radius (nm) *vs.* monomers ratio (St/DVB; 5 : 95 to 95 : 5, v/v). The linear trend-lines serve as guide to the eye.

there were very few PNPs generated when using water-insoluble initiator (Section 3.2.2) and (2) the PNP size decreased with the decrease in temperature (Section 3.2.3). While the IFT mainly determines the size and most importantly the number of NDs created under acoustic irradiation, the solubility of monomer around an emulsion ND is the other key parameter controlling the size of the resulting PNPs. In addition to coagulation of precursor particles or aggregation of water-insoluble oligomers, the particle growth may proceed also *via* a homogeneous mechanism, wherein the NDs present in the system may act as a reservoir of monomers that swell precursor particles or aggregates and are slowly consumed as the polymerization reaction proceeds. Accordingly, a higher content of the less soluble DVB will reduce the overall monomer solubility in the aqueous medium around emulsion NDs, thus disfavoring the growth of large PNPs *via* a homogeneous nucleation mechanism. The solubility values calculated for the systems

of varying St/DVB ratios are given in Table 1; these values are also plotted *vs.* the St/DVB volumetric ratio in Fig. 6b. These data clearly show that an increase in the amount of the less soluble monomer, *viz.* DVB, results in a decrease of the overall solubility of the St/DVB mixture by 80% and also in an increase in IFT by 15% which, ultimately, results in decrease of the PNP radius by 24%.

Alternatively, the solubility of the monomers increases with decreasing the emulsion droplets, due to the higher Laplace pressure, which phenomenon is described by the well-known Kelvin equation:[69]

$$S(r) = S_0 \exp\left(\frac{2\gamma V_m}{rRT}\right) \quad (2)$$

where $S(r)$ is the solubility (mol cm^{-3}) of a particle of radius r (cm), S_0 is the bulk solubility (mol cm^{-3}), γ is the interfacial tension (J cm^{-2}), V_m is the molar volume of the dispersed phase (cm^3), R is the gas constant (8.314 J K^{-1} mol^{-1}), and T is the temperature (300 K).

Eqn (2) shows that a smaller IFT (*i.e.*, γ) leads to a reduced solubility (*i.e.*, S), which is in contrast to the effect observed experimentally in Fig. 6a and c. In order to quantitatively understand this, we have calculated the monomer solubility change due to ND size and IFT with the eqn (2), and included it in the Table 1 and concluded that the latter effect is rather negligible as compared to the effect of the solubility of monomers. It is worth noting that the mechanism proposed by Atobe *et al.* for the tandem acoustic emulsification followed by soap-free emulsion polymerization of MMA[37,41] assumed initiation of polymerization within the emulsified ND, thus affording PNPs of size equal to their ND precursors; the most plausible explanation for the sharp difference between this mechanism and the mechanism suggested in the present system is the maintenance of ultrasonication throughout the polymerization process, which may favor a homogeneous-like nucleation process, and enables the use of less polar monomers, *i.e.* St and DVB.

With the addition of stabilizers, namely 2-SEM, PEG, PVA, the PNP average diameter is larger than 63 nm, which was obtained for the non-stabilized NDs in Fig. 2c, except for the case of CTAB, ~50 nm. The data presented in Fig. 7, shows that the inverse correlation between the monomer/water IFT and PNP sizes continues to hold in the presence of stabilizers. This suggests that the homogeneous-like nucleation mechanism is still dominant even in the presence of 2-SEM, PEG and PVA. In contrast, a dramatically different situation was observed for CTAB. The measured interfacial energy of the monomer oil droplet in the presence of 1% CTAB was by far the lowest, 1.9 mN m^{-1}, yet the resulting PNPs average diameters are the smallest at a mean of 50 nm. The 1% CTAB concentration lies well above the critical micelle concentration of 0.04%, which suggests the possibility of a different polymerization mechanism, *via* micellar

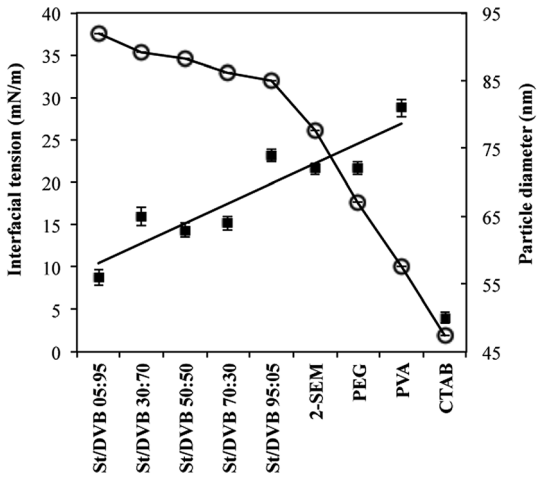

Fig. 7 Emulsion ND/water interfacial tension values (○) and the corresponding size (■) of the final P(St/DVB) NPs, in the absence and in the presence of stabilizers (the trendline was added as guide to the eye).

Table 1 Molecular parameters (at $T = 300$ K) showing that the dependence between emulsion ND size, composition and the total monomer saturated concentration, *i.e.* total monomer availability, in bulk aqueous phase produces a change in the final PNP diameters

St : DVB	IFT[a] (mJ m^{-2})	ND radius[b] (nm)	PNP radius[c] (nm)	Monomer in water[d] (mol cm^{-3})	Monomer in water[e] from eqn (2) (mol cm^{-3})	Change in solubility ΔS (%)	Change in solubility ΔS (%) from eqn (2)	Change in PNP radius ΔR (%)
95 : 5	31.9	66.0	37.2	2.70×10^{-6}	2.82×10^{-6}			
70 : 30	33.0	110.5	32	2.18×10^{-6}	2.24×10^{-6}	−19.41	−20.7	−14
50 : 50	34.6	168.6	31.5	1.72×10^{-6}	1.76×10^{-6}	−36.32	−37.8	−15.3
30 : 70	35.4	199.0	32.6	1.22×10^{-6}	1.25×10^{-6}	−54.65	−55.8	−12.4
5 : 95	37.5	239.9	28.2	5.45×10^{-7}	5.55×10^{-7}	−79.82	−80.4	−24.1

[a] IFT experimentally determined; further details are provided in Section 2.4. [b] Calculated from DLS measurements after 20 min of acoustic emulsification of different mixtures of St/DVB (see Fig. S3 in ESI). [c] Calculated from SEM measurements after polymerization of acoustically emulsified aqueous solutions of St/DVB for 60 min (see Fig. 2). [d] Solubility of the monomer from the monomer mixture, was calculated according to equation $S_{St} = X_{St} \times S_{St(pure)}$,[70] where X is the % molar fraction of the corresponding monomer, $S_{St(pure)} = 2.8 \times 10^{-6}$ mol cm^{-3} and $S_{DVB(pure)} = 0.4 \times 10^{-6}$ mol cm^{-3} in water.[71] The total monomer concentration in the aqueous phase was $X_{St} \times S_{St(pure)} + X_{DVB} \times S_{DVB(pure)}$. [e] Total monomer in water was calculated as a function of ND size by using the Kelvin equation (eqn (2)), where V_m is the molar volume of the St/DVB mixture; the molar volumes of pure monomers $V_{m,St} = 114$ cm^3 and $V_{m,DVB} = 140$ cm^3 were calculated by dividing the molar mass (M) with the density of pure monomers ($\rho_{St} = 0.909$ g cm^{-3}; $\rho_{DVB} = 0.93$ g cm^{-3}).

nucleation, for which the particle size depends on the ratio of the surfactant to the initiator used.[10]

4. Conclusions

We have developed a method for the preparation of poly(styrene-*co*-divinylbenzene) NPs, which involves a one-step acoustic oil-in-water emulsification followed by polymerization of St and DVB monomers under surfactant-free conditions. Optimization of the synthesis method was achieved by fine-tuning different reaction parameters, including the total concentration of the monomer/crosslinker and their relative ratio, the nature and the concentration of the initiator, the reaction temperature and time. Under these optimized conditions, P(St/DVB) NPs could be isolated at a yield of 8.5%, free of surfactants or stabilizers. We have shown that the ultrasonication can drive the polymerization reaction and prevent the aggregation of the formed PNPs.

The size of the PNPs obtained depends: (i) inversely on the monomer/water interfacial energy and emulsification power, and (ii) directly on temperature, amount of initiator and monomer solubility. These experimental observations indicate that a coagulative nucleation mechanism (homogeneous nucleation followed by coagulation of growing particles and swelling with unreacted monomer) is predominant. The same mechanism can also be hypothesized in the presence of interfacial stabilizers. One notable exception was observed for the case of CTAB surfactant, for which a micellar nucleation mechanism is more likely. A secondary effect of stabilizers was that the particle-diameter dispersity and shape was improved especially in the presence of a co-polymerizable surfactant monomer, 2-SEM.

Acknowledgements

We are especially grateful for the financial support of Metrohm Foundation (Herisau, Switzerland) and of ZHAW *via* Anschubfinanzierung. We also acknowledge funding from NTU iFood Research Grant (M4081465.120) and Singapore Ministry of Education Academic Research Fund Tier 2 (MOE2014-T2-2-074).

References

1 S. Bamrungsap, Z. Zhao, T. Chen, L. Wang, C. Li, T. Fu and W. Tan, *Nanomedicine*, 2012, **7**, 1253–1271.
2 M. R. Gonçalves, *J. Phys. D: Appl. Phys.*, 2014, **47**, 213001.
3 A. M. Coto-García, E. Sotelo-González, M. T. Fernández-Argüelles, R. Pereiro, J. M. Costa-Fernández and A. Sanz-Medel, *Anal. Bioanal. Chem.*, 2011, **399**, 29–42.
4 M. Ballauff and Y. Lu, *Polymer*, 2007, **48**, 1815–1823.
5 G. J. Nohynek and E. K. Dufour, *Arch. Toxicol.*, 2012, **86**, 1063–1075.
6 X. Yu and V. M. Rotello, *Nat. Nanotechnol.*, 2011, **6**, 693–694.
7 R. Nagarajan, in *Nanoparticles: Synthesis, Stabilization, Passivation, and Functionalization*, American Chemical Society, 2008, vol. 996, pp. 2–14.
8 *Nanoparticles: From Theory to Application*, ed. G. Schmidt, Wiley-VCH Verlag GmbH & Co. KGaA, Weinheim, 2nd edn, 2010.
9 *Advanced Polymer Nanoparticles: Synthesis and Surface Modifications*, ed. V. Mittal, Boca Raton, FL, CRC Press., 2011.
10 C.-S. Chern, in *Principles and Applications of Emulsion Polymerization*, John Wiley & Sons, Inc., New Jersey, 2008.
11 J. C. Garay-Jimenez, A. Young, D. Gergeres, K. Greenhalgh and E. Turos, *Nanomedicine Nanotechnol. Biol. Med.*, 2008, **4**, 98–105.
12 R. H. Ottewill and J. N. Shaw, *Kolloid Z. Z. Polym.*, 1967, **215**, 161–166.
13 K. Chen, Y. Zhu, Y. Zhang, L. Li, Y. Lu and X. Guo, *Macromolecules*, 2011, **44**, 632–639.
14 J. C. Garay-Jimenez and E. Turos, *Bioorg. Med. Chem. Lett.*, 2011, **21**, 4589–4591.
15 M. Pan, L. Yang, B. Guan, M. Lu, G. Zhong and L. Zhu, *Soft Matter*, 2011, **7**, 11187.
16 T. S. Skelhon, Y. Chen and S. A. F. Bon, *Langmuir*, 2014, **30**, 13525–13532.
17 N. Schöler, C. Olbrich, K. Tabatt, R. H. Müller, H. Hahn and O. Liesenfeld, *Int. J. Pharm.*, 2001, **221**, 57–67.
18 R. Ferrari, C. Colombo, C. Casali, M. Lupi, P. Ubezio, F. Falcetta, M. D'Incalci, M. Morbidelli and D. Moscatelli, *Int. J. Pharm.*, 2013, **453**, 551–559.
19 S. E. Shim, S. Yang, M.-J. Jin, Y. H. Chang and S. Choe, *Colloid Polym. Sci.*, 2004, **283**, 41–48.
20 S. E. Shim, S. Yang, H. H. Choi and S. Choe, *J. Polym. Sci., Part A: Polym. Chem.*, 2004, **42**, 835–845.
21 H. Cui, H. Chen, R. Qu, C. Wang, C. Sun, W. Zhou, M. Yu and H. Jiang, *J. Appl. Polym. Sci.*, 2009, **111**, 3144–3149.
22 H. Jiang, H. Chen, G. Zong, X. Liu, Y. Liang and Z. Tan, *Polym. Adv. Technol.*, 2011, **22**, 2096–2103.
23 Z. Tan, J. Ma, H. Chen, N. Ji and G. Zong, *J. Appl. Polym. Sci.*, 2012, **124**, 3799–3806.
24 M. Bradley and F. Grieser, *J. Colloid Interface Sci.*, 2002, **251**, 78–84.
25 G. Franz and M. Ashokkummar, in *Colloids and Colloid Assemblies*, ed. F. Caruso, Wiley-VCH Verlag GmbH & Co. KGaA, Weinheim, 2004, p. 603.
26 M. Nakanishi, H. Takatani, Y. Kobayashi, F. Hori, R. Taniguchi, A. Iwase and R. Oshima, *Appl. Surf. Sci.*, 2005, **241**, 209–212.
27 J.-E. Park, M. Atobe and T. Fuchigami, *Electrochim. Acta*, 2005, **51**, 849–854.
28 V. Sáez and T. J. Mason, *Molecules*, 2009, **14**, 4284–4299.
29 B. Küçük, N. Özkan and M. Volkan, *J. Phys. Chem. Solids*, 2013, **74**, 1426–1432.
30 J. H. Bang and K. S. Suslick, *Adv. Mater.*, 2010, **22**, 1039–1059.
31 H. Xu, B. W. Zeiger and K. S. Suslick, *Chem. Soc. Rev.*, 2013, **42**, 2555–2567.
32 M. K. Li and H. S. Fogler, *J. Fluid Mech.*, 1978, **88**, 499–511.
33 M. K. Li and H. S. Fogler, *J. Fluid Mech.*, 1978, **88**, 513–528.
34 S. R. Reddy and H. S. Fogler, *J. Phys. Chem.*, 1980, **84**, 1570–1575.
35 T. Sakai, *Curr. Opin. Colloid Interface Sci.*, 2008, **13**, 228–235.

36 K. Nakabayashi, F. Amemiya, T. Fuchigami, K. Machida, S. Takeda, K. Tamamitsu and M. Atobe, *Chem. Commun.*, 2011, **47**, 5765–5767.
37 K. Nakabayashi, M. Kojima, S. Inagi, Y. Hirai and M. Atobe, *ACS Macro Lett.*, 2013, **2**, 482–484.
38 K. Nakabayashi, H. Yanagi and M. Atobe, *RSC Adv.*, 2014, **4**, 57608–57610.
39 T. Sakai, H. Sakai and M. Abe, *Langmuir*, 2002, **18**, 3763–3766.
40 C. Zhang, Q. Wang, H. Xia and G. Qiu, *Eur. Polym. J.*, 2002, **38**, 1769–1776.
41 Y. Hirai, K. Nakabayashi, M. Kojima and M. Atobe, *Ultrason. Sonochem.*, 2014, **21**, 1921–1927.
42 L. H. Thompson and L. K. Doraiswamy, *Ind. Eng. Chem. Res.*, 1999, **38**, 1215–1249.
43 S. Slomkowski, J. V. Alemán, R. G. Gilbert, M. Hess, K. Horie, R. G. Jones, P. Kubisa, I. Meisel, W. Mormann, S. Penczek and R. F. T. Stepto, *Pure Appl. Chem.*, 2011, **83**, 2229–2259.
44 S. Mujumdar, P. Senthil Kumar and A. B. Pandit, *Indian J. Chem. Technol.*, 1997, **4**, 277–284.
45 C. Walling, E. R. Briggs and F. R. Mayo, *J. Am. Chem. Soc.*, 1946, **68**, 1145–1149.
46 G. Goldfinger and K. E. Lauterbach, *J. Polym. Sci.*, 1948, **3**, 145–156.
47 P. Kruus, *Ultrasonics*, 1983, **21**, 201–204.
48 L. A. Dupont, P. Kruus and T. J. Patraboy, in *Ultrasonics International 83*, Butterworth & Co. Ltd, Borough Green, UK, 1983, pp. 502–506.
49 P. Kruus, D. McDonald and T. J. Patraboy, *J. Phys. Chem.*, 1987, **91**, 3041–3047.
50 C. E. Harland, *Ion Exchange*, The Royal Society of Chemistry, 1994.
51 A. R. Goodall, M. C. Wilkinson and J. Hearn, *J. Polym. Sci., Polym. Chem. Ed.*, 1977, **15**, 2193–2218.
52 J. W. Goodwin, J. Hearn, C. C. Ho and R. H. Ottewill, *Br. Polym. J.*, 1973, **5**, 347–362.
53 G. T. D. Shouldice, G. A. Vandezande and A. Rudin, *Eur. Polym. J.*, 1994, **30**, 179–183.
54 P. J. Feeney, D. H. Napper and R. G. Gilbert, *Macromolecules*, 1987, **20**, 2922–2930, and references cited therein.
55 J. W. Goodwin, J. Hearn, C. C. Ho and R. H. Ottewill, *Colloid Polym. Sci.*, 1974, **252**, 464–471.
56 R. Büttiker, J. Ebert, C. Hinderling and C. Adlhart, *Clin. Chim. Acta*, 2011, **65**, 182–186.
57 C. Wu, *Macromolecules*, 1994, **27**, 298–299.
58 C. Wu, *Macromolecules*, 1994, **27**, 7099–7102.
59 A. Kotera, K. Furusawa and Y. Takeda, *Kolloid Z. Z. Polym.*, 1970, **239**, 677–681.
60 A. Kotera, K. Furusawa and K. Kudō, *Kolloid Z. Z. Polym.*, 1970, **240**, 837–842.
61 F. K. Hansen and J. Ugelstad, *J. Polym. Sci., Polym. Chem. Ed.*, 1979, **17**, 3033–3045.
62 M. Chainey, J. Hearn and M. C. Wilkinson, *J. Polym. Sci., Part A: Polym. Chem.*, 1987, **25**, 505–518.
63 Z. Song and G. W. Poehlein, *J. Colloid Interface Sci.*, 1989, **128**, 501–510.
64 I. Kühn and K. Tauer, *Macromolecules*, 1995, **28**, 8122–8128.
65 S. Peach, *Macromolecules*, 1998, **31**, 3372–3373.
66 K. Tauer, R. Deckwer, I. Kühn and C. Schellenberg, *Colloid Polym. Sci.*, 1999, **277**, 607–626.
67 C. S. Chern, *Prog. Polym. Sci.*, 2006, **31**, 443–486, and references cited therein.
68 A. M. Telford, B. T. T. Pham, C. Neto and B. S. Hawkett, *J. Polym. Sci., Part A: Polym. Chem.*, 2013, **51**, 3997–4002.
69 T. F. Tadros, E. Vandekerckhove, M. Lemmens, B. Levecke and K. Booten, in *Emulsion Science and Technology*, ed. Tharwat F. Tadros, WILEY-VCH Verlag GmbH & Co. KGaA, Weinheim, 2009, pp. 57–66.
70 S. Banerjee, *Environ. Sci. Technol.*, 1984, **18**, 587–591.
71 DHHS (NIOSH), *NIOSH Pocket Guide Chem. Hazards Educ. Inf. Div*.